
Effect of voxel size in flow direction on permeability and Forchheimer coefficients determined by using micro-tomography images of a porous medium

Eren Ucar

Mechanical Engineering Department,
Izmir Institute of Technology,
35430 Urla, Izmir, Turkey
and
Department of Mathematics,
University of Bergen,
5007 Bergen, Norway
E-mail: eren.ucar@math.uib.no

Moghtada Mobedi*

Mechanical Engineering Department,
Izmir Institute of Technology,
35430 Urla, Izmir, Turkey
E-mail: moghtadamobedi@iyte.edu.tr
*Corresponding author

Gokhan Altintas

Department of Mechanical Sciences,
Engineering Faculty,
Celal Bayar University,
45100 Muradiye, Turkey
E-mail: gokhanaltintas@gmail.com

Erik Glatt

Fraunhofer-Institut für Techno-und Wirtschaftsmathematik,
67663 Kaiserslautern, Germany
E-mail: erik.glatt@math2market.de

Abstract: The permeability and Forchheimer coefficients of a porous medium, volcanic rock, are determined using micro-tomography images. A cubic volume in the middle of the images is extracted as REV (representative volume). The voids in the REV are discretised into anisotropic voxels using the commercial program of GeoDict. Seven computational domains with different voxel size in flow direction are generated. The velocity and pressure fields in the voids are obtained for Reynolds numbers ranging from 0.01 to 10. The obtained fields are used to determine the permeability and the Forchheimer coefficients. The performed calculations show that the nominal pore size changes with the voxel size in flow direction, however permeability and the Forchheimer coefficient approaches to the constant values.

Keywords: porous media; tomography; permeability; Forchheimer.

Reference to this paper should be made as follows: Ucar., E., Mobedi, M., Altintas, G. and Glatt, E. (2015) 'Effect of voxel size in flow direction on permeability and Forchheimer coefficients determined by using micro-tomography images of a porous medium', *Progress in Computational Fluid Dynamics*, Vol. 15, No. 5, pp.327–333.

Biographical notes: Eren Ucar received both her BSc and MSc degrees in Mechanical Engineering from Izmir Institute of Technology, Turkey. She is currently a PhD student in the Department of Mathematics, University of Bergen, Norway. Her research work concerns numerical analysis of heat and fluid flow in porous media together with modelling and simulation of geothermal reservoirs.

Moghtada Mobedi is an Associate Professor in the Mechanical Engineering Department of Izmir Institute of Technology, Turkey. He received his PhD degree from the Middle East Technical University in 1994. His research interests include computational heat transfer, heat and fluid flow in porous media and heat and mass transfer in adsorbent beds. Recently, his interests are on the determination of macroscopic transport properties of porous media such as permeability, Forchheimer coefficient, interfacial heat transfer and thermal dispersion coefficients from the microscopic fields of velocity, pressure and temperature.

Gokhan Altintas received his BS in Civil Engineering from Dokuz Eylul University, Turkey, in 1992, his MS degree from Celal Bayar University, Turkey, in 1996, where he is currently working as an Associate Professor, and his PhD in Vibration Mechanics in Civil Engineering from Yildiz Technical University, Turkey, in 2002. His research interests include: modal analysis, voxel-based finite element methods, computer simulations and reverse engineering problems.

Erik Glatt received his Master's degree and his PhD in Physics from the Technische Universität Darmstadt. After finishing his PhD degree, he joined the Fraunhofer Institute for Industrial Mathematics (ITWM) in Kaiserslautern, Germany, in 2008. At ITWM, he worked on random 3D-material models and image-based material property computations. Since 2011, he is the co-founder and Chief Technology Officer of Math2Market, where he is in charge of scientific and technological aspects of product definition and development, and the management of projects and systems.

This paper is a revised and expanded version of a paper entitled 'Effect of slice step size on tomography based determination of permeability in a porous medium' presented at the InterPore2013 Conference, Prague, 21–24 May 2013.

1 Introduction

Recent developments on imaging technique such as computer tomography provide not only 3D observation of pores in particles but also determination of macroscopic properties of a porous medium by using direct pore level simulation (DPLS). Several studies were reported in literature on the determination of macroscopic transport properties of a real porous medium by using tomography images. For instance, [Akolkar and Petrasch \(2012\)](#) investigated two kinds of porous media as reticulated porous ceramic foam and packed bed of CaCO_3 particles by using DPLS and the permeability and the Dupuit-Forchheimer coefficients were determined. [Fourar et al. \(2005\)](#) investigated the inertia effects in high-rate flow through heterogeneous porous media of serial-layers, parallel-layers and correlated. The theoretical relationships were proposed for the inertial coefficient as function of the Reynolds number and the characteristics of the porous media. [Peszynska and Trykozko \(2011\)](#) solved Navier-Stokes equations in complex pore geometries and obtained the average of the achieved results to derive flow properties based on non-Darcy flow model. They ([Peszynska and Trykozko, 2013](#)) also performed another study on pore-to-core simulations of flow with large velocities using continuum models and imaging data. They found that the difference in conductivities between body fitting grid and voxel-based grids are 10%. [Balhoff and Wheeler \(2009\)](#) obtained the permeability and non-Darcy

coefficient for the isotropic and anisotropic porous media for both computer-generated porous media and real sandstones digitised through x-ray computed microtomography where Forchheimer equation is applicable.

Literature survey showed that CFD programs are used in all of the reported studies in this field in order to determine velocity and pressure distributions in digitised porous media, and this requires high number of grids and computational time to obtain accurate results. The use of anisotropic voxels in flow direction may be a solution to reduce computational time however its effect on the obtained computational results should be investigated. In this study, the velocity and pressure distributions of air through a volcanic rock sample are obtained by using images of micro-tomography. Then, the values of permeability and Forchheimer coefficients are calculated based on the achieved results. Two commercial software, one for generation of voxels for the domain and the other for solving continuity and momentum equations based on finite volume method are employed. The aim of study is to investigate the effects of longitudinal size of voxels (or anisotropic voxel effect) on the velocity and pressure distributions and furthermore on the permeability and Forchheimer coefficients of a porous medium.

2 Micro-tomography images of the porous medium

Figure 1(a) shows the volcanic rock sample considered in this study. The sample originally has a cylindrical shape with length and diameter of 7.907 and 11.470 mm, respectively. Micro-computer tomography of this material was carried out to construct 3D pore level digital representation. The 3D volume rendering of the volcanic rock obtained by GeoDict (Math2 Market GmbH, 2013) software can be seen in Figure 1(b). Each slice has $4,000 \times 4,000$ pixels and the distance between two slices is $3.23 \mu\text{m}$. The region of interest with $400 \times 400 \times 150$ pixels ($1,292 \times 1,292 \times 484.5 \mu\text{m}$) was extracted from the centre of the received images. A representative image of the computational domain is shown in Figure 1(c). The computational domain consists of a square duct containing a layer of the porous material at the middle and clear fluid regions at inlet and outlet to provide the natural behaviour of the flow at the inlet and outlet of porous layer. Air at 300 K was selected as working fluid.

3 Microscopic and macroscopic governing equations

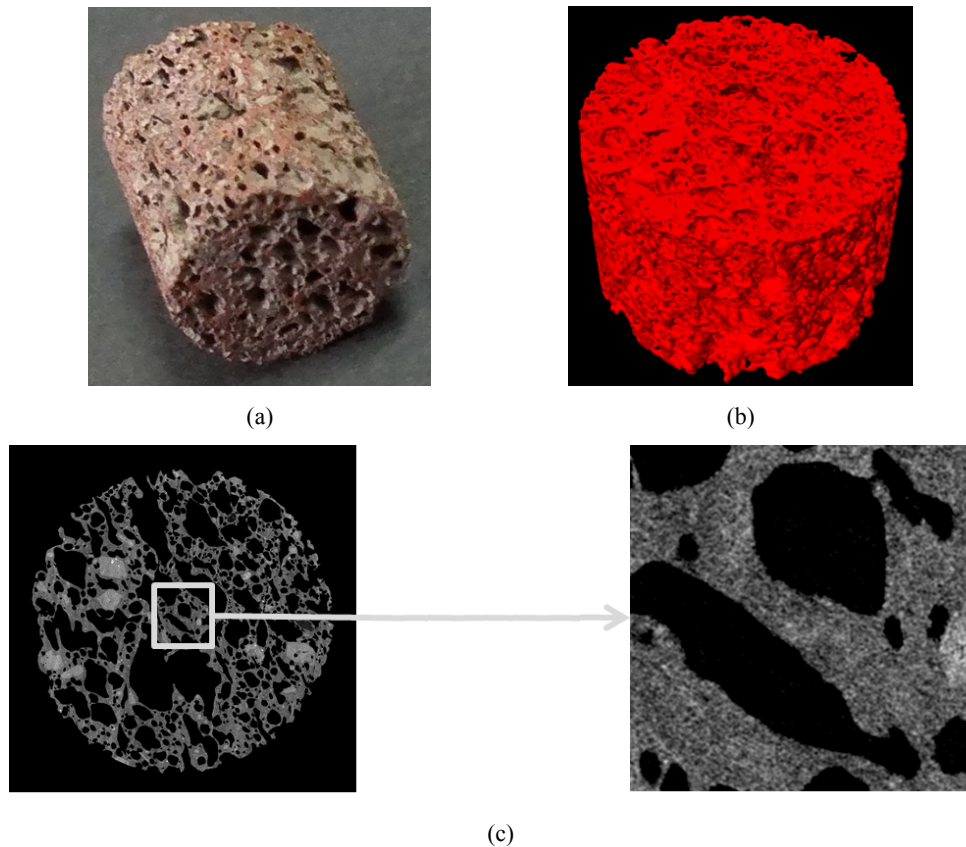
The flow in the voids of the porous medium is assumed steady, Newtonian and incompressible. The microscopic governing equations are continuity and momentum equations as:

$$\vec{\nabla} \cdot \vec{V} = 0 \quad (1)$$

$$\vec{V} (\vec{\nabla} \cdot \vec{V}) = -\frac{1}{\rho} \vec{\nabla} p + \nu \vec{\nabla}^2 \vec{V} \quad (2)$$

where \vec{V} , p , ρ and ν are velocity vector, pressure, density and kinematic viscosity of fluid, respectively. For the considered computational domain, the boundary conditions are uniform inlet velocity for inlet boundary surface, specified pressure for the outlet and no-slip at the solid–fluid interface.

Figure 1 Different views of the considered volcanic rock, (a) studied volcanic rock sample (b) 3D volume rendering of the sample (c) region of interest extracted from the centre of the received images (see online version for colours)



The fluid particles have three directional motions in the porous medium. However; the flow through the porous medium can be considered as unidirectional from the macroscopic point of view. The Darcy's Law for 1D problem can be expressed as,

$$\langle u \rangle = -\frac{K}{\mu} \frac{d\langle p \rangle^f}{dx} \quad (3)$$

where $\langle u \rangle$, μ and K are Darcy velocity, dynamic viscosity and permeability, respectively. An additional quadratic term was proposed by Dupuit and Forchheimer for fluid flows with high particle-based Reynolds numbers called as Forchheimer extended Darcy's Law:

$$-\frac{d\langle p \rangle^f}{dx} = \frac{\mu}{K} \langle u \rangle + \frac{C}{\sqrt{K}} \rho_f (\langle u \rangle)^2 \quad (4)$$

where C is Forchheimer constant. Non-dimensionalisation of equation (4) for the one-dimensional flow in a channel can be found as:

$$-\frac{d_{nom}^2}{\langle u \rangle \mu_f} \frac{d\langle p \rangle^f}{dx} = \frac{d_{nom}^2}{K} + C \left(\frac{d_{nom}^2}{K} \right)^{1/2} \text{Re} \quad (5)$$

where d_{nom} is the nominal diameter and Re can be defines as

$$\text{Re} = \rho_f \langle u \rangle d_{nom} / \mu_f.$$

The nominal diameter, d_{nom} , used throughout this study is calculated by the help of pore size distributions with following formula,

$$d_{nom} = \sum_{i=1}^n d_i X_i \quad (6)$$

where d_i is the pore diameter and X_i is the fraction of the pore diameter. For simplicity, equation (5) can be expressed as,

$$\Pi = a + b \text{Re} \quad (7)$$

where $\Pi = -\frac{d_{nom}^2}{\langle u \rangle \mu_f} \frac{d\langle p \rangle^f}{dx}$ is the dimensionless pressure

gradient, a is the inverse dimensionless permeability, $\frac{d_{nom}^2}{K}$

and $b = C \left(\frac{d_{nom}^2}{K} \right)^{1/2}$.

4 Solution and upscaling methods

In order to determine the permeability and Forchheimer coefficients by using microtomography images, three steps should be followed. In the first step, microtomography images should be processed to obtain the digital representation of the considered porous medium. Then, the pressure drop and velocity fields in the considered porous domain should be obtained by solving continuity and

momentum equations. Finally, the average velocity and pressure drop in the cross section at different locations in flow direction of the porous medium should be calculated. The values of K and F can be calculated by upscaling of the results means taking space average of the local results and then adapting the averaged results to the Forchheimer extended Darcy's Law.

In this study, the micro-tomography images of the considered sample were imported to the GeoDict software. The volume rendering, the pore diameter distribution and voxel-based mesh for the considered sample were obtained by using GeoDict software. Following, a commercial CFD code as ANSYS Fluent 14.0 (ANSYS Inc., 2011) written based on the finite volume technique was used to solve the continuity and Navier–Stokes equations. Hence, the velocity and pressure drop distributions along the channel consists of three parts as inlet, porous and outlet regions were found. The convergence criterion as 10^{-7} was used to terminate iterations in Fluent software. To observe the pressure drop in flow direction through the channel, several cross sections perpendicular to the flow direction were created. The intrinsic average of pressure for each cross section area was obtained by area weighted integral of pressure in the fluid region. There is no doubt that the Darcy velocity is the same with uniform velocity at the inlet boundary and its value was changed 0.001 to 0.85 m/s.

5 Results and discussion

The flow computation on the original domain with $400 \times 400 \times 150$ voxels is very costly with regards to the computational time and the required amount of RAM. That is why, anisotropic voxels are used. The original porous region was reduced to $400 \times 400 \times 5$ pixels by removing 32 images between each 33 images. The velocity and pressure distributions for $400 \times 400 \times 5$ pixels domain was obtained. By the same way, the pore level governing equations were solved for the domains having $400 \times 400 \times 10$, $400 \times 400 \times 18$, $400 \times 400 \times 38$, $400 \times 400 \times 76$ pixels. Based on equation (6), the nominal pore diameter of the generated computational domains can be seen in Table 1. The calculated nominal pore diameters are almost the same for all generated domains except for $400 \times 400 \times 38$. This figure shows that the pore distribution changes with number of images in flow direction.

Table 1 The change of nominal pore diameter with number of images in flow direction

Number of images in flow direction	Nominal pore diameter (μm)
5	171.84
10	171.12
18	198.20
38	200.77
76	164.85

The velocity and pressure distributions in the voids for the studied domains are also observed and analysed in this study. The planes are created along the flow direction to observe the velocity and pressure distributions. As an example, the velocity and pressure distributions for the domain of $400 \times 400 \times 18$ when the inlet velocity is 0.005 m/s are shown in Figure 2. Air enters to the computational domain with uniform velocity and passes through the porous medium. For some part of the presented figure, air cannot move in flow direction (Z direction) and

collide to the solid. Consequently, the direction of flow changes to other directions (Y and/or X directions). Secondary flows are also observed especially at the outlet region due to jet effect at the outlet of the pores. As can be seen from Figure 2(b), which shows the pressure distribution through the porous media, air flows from high pressure to low pressure. However, no uniform pressure drop through the channel is observed due to secondary flows occur in some voids.

Figure 2 The velocity and pressure distributions in a plane created in the flow direction of the domain $400 \times 400 \times 18$ pixels for inlet velocity of 0.005 m/s , (a) velocity distribution (b) pressure distribution (see online version for colours)

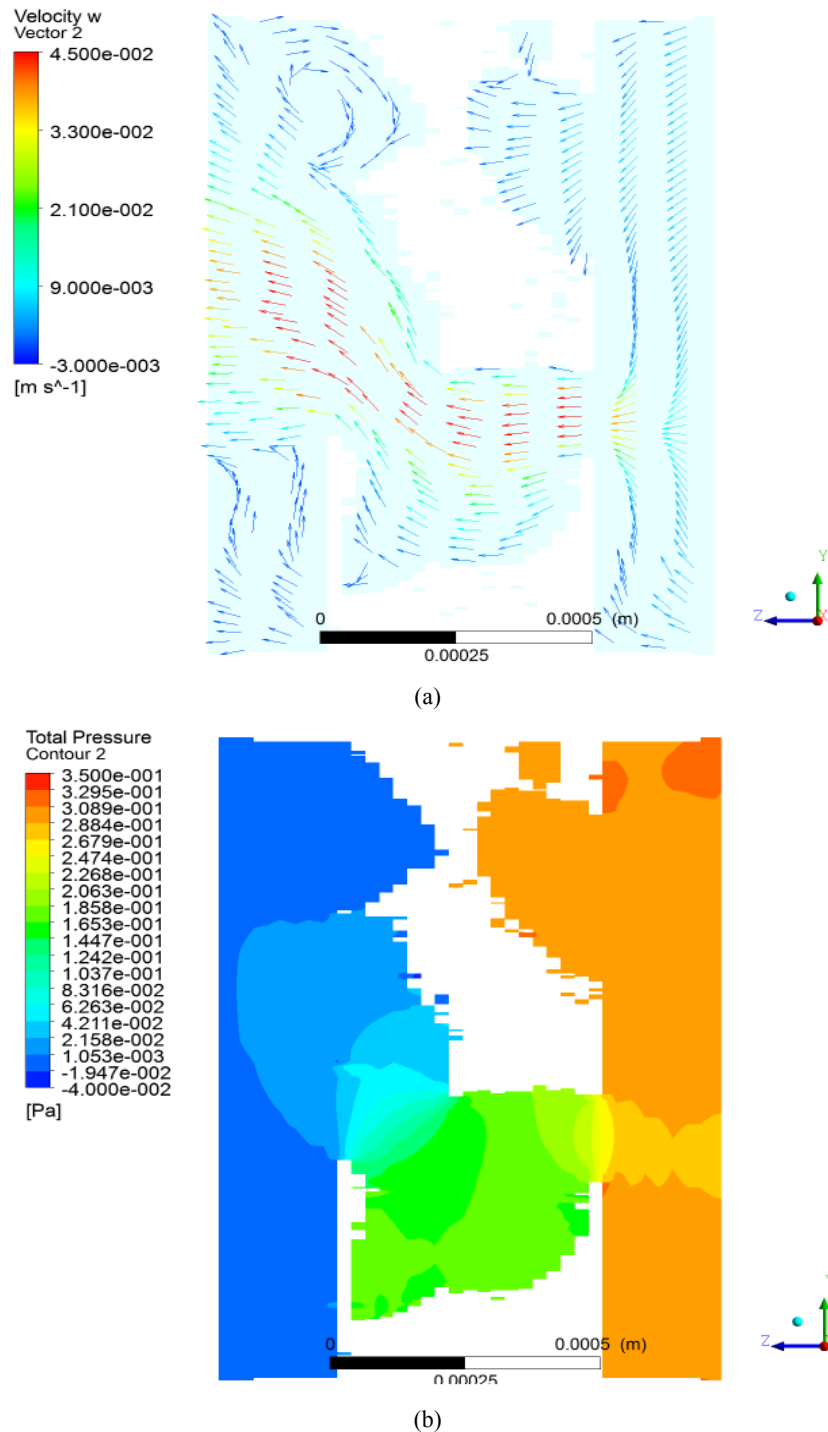


Figure 3 The dimensionless averaged pressure profile for the domain $400 \times 400 \times 18$ pixels

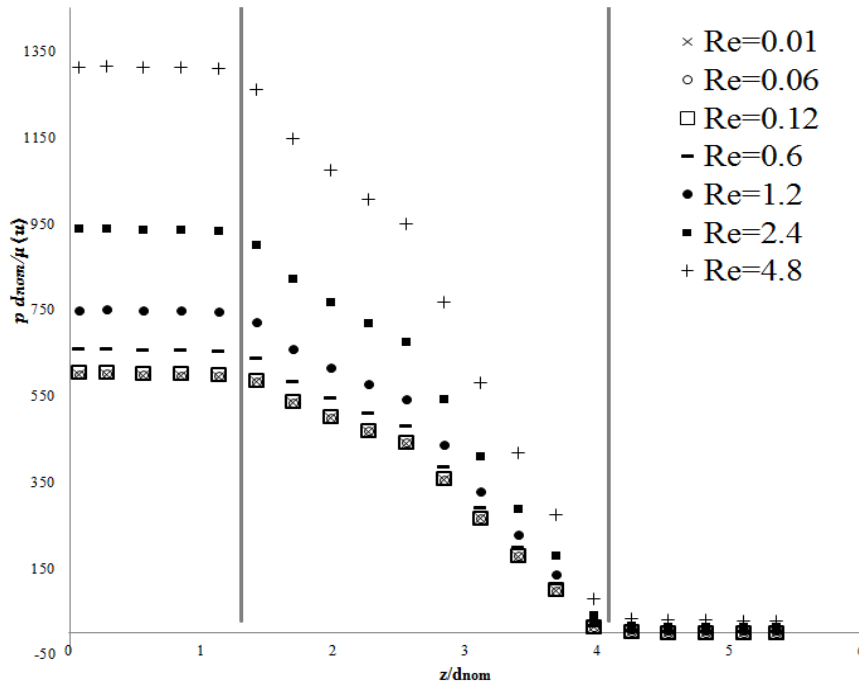
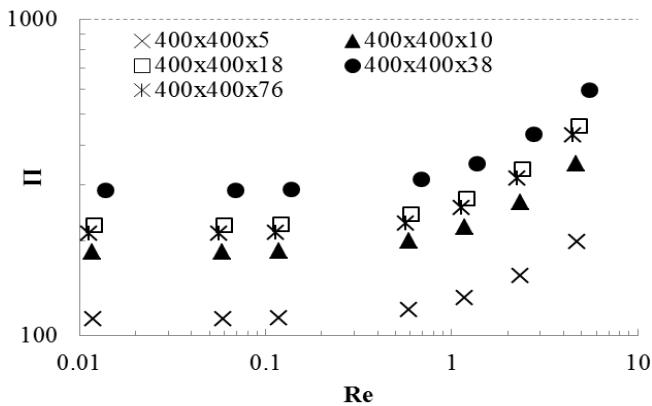


Figure 3 shows the change of dimensionless averaged pressure profile (i.e., upscaled pressure profile) along the direction of the flow for the domain of $400 \times 400 \times 18$ pixels and for different values of Re numbers. As expected, the dimensionless averaged pressures are almost constant for the inlet and outlet regions due to flow in clear regions. The dimensionless averaged pressures start to decrease dramatically from the beginning of the porous structure for all Re numbers. The curves belong to the low Re numbers (i.e., $Re = 0.01, 0.05, 0.12$) overlap each other indicating flow is in the Darcy region. As Re number increase, the inertia terms takes important role and the pressure profiles separates from each other.

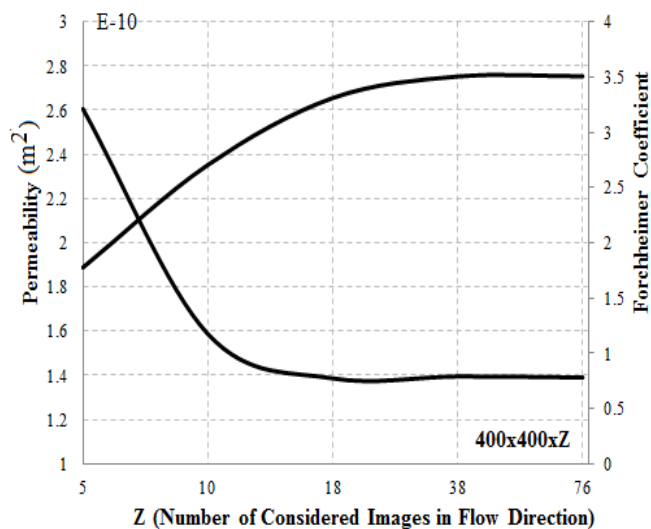
Figure 4 The dimensionless pressure gradient for the domain $400 \times 400 \times 18$ pixels



The changes of the dimensionless pressure gradient with Re numbers for considered computational domains are plotted and shown in Figure 4. As expected, the dimensionless pressure gradient is constant for low Reynolds number (i.e., $Re < 0.5$). After a specified value of Reynolds number, the value of Π increases with Re number due to inertia effect. By increase of image number, the distributions of pressure with Reynolds number become closer to each other. However, it is observed that, the values of dimensionless pressure of the domain with $400 \times 400 \times 38$ pixels diverge from the other domains because of the deviation of the nominal pore diameter for this domain. The dimensionless parameters of equation (7), namely a and b , can be calculated by using obtained results. The value of ' a ' represents the dimensionless pressure gradient for the flow in Darcy region, while ' $b * Re$ ' shows the dimensionless pressure gradient for the flows in which the inertia effect is completely dominant.

The change of permeability for the computed domains (i.e., number of image in flow direction) can be seen in Figure 5. The permeability value decreases with the increase of image number in flow direction. The permeability values converge to a constant value by further increase of the image number in flow direction in spite of small changes of nominal pore diameter. The final value of permeability is $1.4 \times 10^{-10} \text{ m}^2$ for the considered region of interest. The Forchheimer coefficient increases with the increase of image number in the flow direction. After a point, the Forchheimer coefficient converges to a constant value which is 3.5.

Figure 5 The change of permeability and Forchheimer coefficient with number of image in flow direction



6 Conclusions

The micro-tomography images are employed to represent a real porous media (volcanic rock sample) in computer. The effects of the voxel size in flow direction on the flow field, permeability and Forchheimer coefficients are analysed. Based on the obtained results, following remarks can be concluded:

- Removing of images in flow direction generates anisotropic voxels, decreases number of voxels considerably and reduces computational time.
- The nominal pore diameters changes with the change of anisotropic voxel size. Hence, the dimensionless permeability and Reynolds number vary with size of voxels.

- For the studied porous medium, both the permeability and Forchheimer coefficients approach to the constant values by decreasing of voxel size in flow direction.
- For a REV in the centre of the studied volcanic rock, the predicted value of permeability and Forchheimer coefficient are obtained as $1.4 \times 10^{-10} \text{ m}^2$ and 3.5, respectively.

The permeability is a tensor quantity and further studies on the effect of voxel size in flow direction should be performed to investigate the variation of the other components of the permeability tensor with number of image in flow direction.

References

- Akolkar, A. and Petrasch, J. (2012) 'Tomography-based characterization and optimization of fluid flow through porous media', *Transport in Porous Media*, Vol. 95, No. 3, pp.535–550.
- ANSYS Inc. (2011) *ANSYS Fluent User's Guide 14.0*, USA.
- Balhoff, M. and Wheeler, M.F. (2009) 'A predictive pore-scale model for non-Darcy flow in porous media', *Society of Petroleum Engineers Journal*, Vol. 14, No. 4, pp.579–587.
- Fourar, M., Lenormand, R., Karimi-Fard, M. and Horne, R. (2005) 'Inertia effects in high-rate flow through heterogeneous porous media', *Transport in Porous Media*, Vol. 60, No. 3, pp.353–370.
- Math2 Market GmbH (2013) *GeoDict User's Guide*, Kaiserslautern, Germany.
- Peszynska, M. and Trykozko, A. (2013) 'Pore-to-core simulations of flow with large velocities using continuum models and imaging data', *Computational Geosciences*, Vol. 17, No. 4, pp.623–645.
- Peszynska, M. and Trykozko, A. (2011) 'Convergence and stability in upscaling of flow with inertia from Pore scale to mesoscale', *International Journal for Multiscale Computational Engineering*, Vol. 9, No. 3, pp.215–229.